Dynamical properties of a diffusion-limited cluster - cluster aggregation model

1996 J. Phys.: Condens. Matter 8 5555

(http://iopscience.iop.org/0953-8984/8/30/006)

J. Phys.: Condens. Matter **8** (1996) 5555–5567. Printed in the UK

Dynamical properties of a diffusion-limited cluster–cluster aggregation model

Abdelali Rahmani†‖, Claude Benoit‡, Rémi Jullien§, Gérard Poussigue‡ and Abdellah Sakout†

† Laboratoire d'Optique et de Spectroscopie, Faculté des Sciences, Dhar Mehraz, BP 1796 Atlas-Fès, Morocco

‡ Groupe de Dynamique des Phases Condensées, UMR 5581 CNRS, Université Montpellier II, CP026 Place Eugène Bataillon, 34095 Montpellier Cédex 5, France¶

§ Laboratoire de Science des Matériaux Vitreux, UMR 5587 CNRS, Université Montpellier II, Place Eugène Bataillon, 34095 Montpellier Cédex 5, France

Received 20 October 1995, in final form 14 March 1996

Abstract. In order to test the validity of the dynamical scaling arguments put forward by Alexander, Courtens and Vacher in 1993 without a specific model, we previously published results concerning percolation clusters (in 1995). In the present paper, for the first time, we have extended calculations to the diffusion-limited cluster aggregation (DLCA) model, in three dimensions (3D). There was excellent agreement with the theory, better than in the percolation case. The density of states and dynamic structure factor are calculated for the very large 3D DLCA model using the spectral moments method. The results are analysed in terms of scaling theory and compared to experimental results concerning silica aerogels.

1. Introduction

Highly ramified fractal aggregates have recently attracted considerable interest, partly because of their potential for describing a wide range of non-regular structures, ranging from colloids and polymer gels to galactic structures. Jullien and Botet (1987) have recently developed a model for diffusion-limited cluster–cluster aggregation (DLCA) which produces random structures close to those observed in nature (Meakin 1983, Kolb *et al* 1983). Numerical simulations indicate that the latter structures have remarkable scaling and universal properties (Botet *et al* 1983, Jullien and Botet 1987, Hasmy *et al* 1993, 1994). The fractal dimension of DLCA built in three dimensions ($D = 1.78$) is much smaller than the Euclidean one ($d = 3$). These models are basically used to obtain a better understanding of real colloidal aerogels (Foret 1992).

Dynamical scaling has been applied to the dynamics of fractal structures. To test the validity of such predictions, there have been many comparisons of experimental results obtained on silica aerogels (Courtens *et al* 1987, 1988, Vacher *et al* 1988, 1990, Tsujimi *et al* 1988, Reichenauer *et al* 1989), which were shown to be fractal, and of numerical results mostly concerning scalar elasticity models for percolation clusters (Montagna *et al* 1990, Russ *et al* 1991, Stoll *et al* 1992, Nakayama and Yakubo 1992, Nakayama *et al* 1994,

‖ Permanent address: Département de Physique, Université Kaddi Ayad, Faculté des Sciences et Techniques, BP 618, Gheliz-Marrakech, Morocco.

¶ Mailing address.

0953-8984/96/305555+13$19.50

Rahmani *et al* 1995). The aim of this paper is to test the validity of dynamical scaling assumptions with respect to the 3D DLCA model.

As first pointed out by Alexander and Orbach (1982), thermal excitation spectra are strongly influenced by the fractal structure. To describe the vibrational density of states (DOS) $g(\omega)$ of these systems, Alexander and Orbach introduced the spectral dimension $\tilde{d}$ for fracton modes:

$$g(\omega) \approx \omega^{\tilde{d}-1}. \tag{1}$$

In homogeneous systems, $\tilde{d}$ corresponds to the Euclidean dimension d.

To obtain further information on the dynamics of fractal structures, Alexander (1989) and Alexander *et al* (1993) studied the dynamic structure factor $S(\boldsymbol{q}, \omega)$ of these systems without any specific structure model. Based on the single-length-scale postulate (SLSP), they showed that $S(\boldsymbol{q}, \omega)$ should have the following scaling form, depending only on the single length scale $\lambda(\omega) \approx \omega^{-\tilde{d}/D}$:

$$S(q, \omega) = q^{y} H(q\lambda(\omega)) \tag{2}$$

where H is a scaling function and $q = |\boldsymbol{q}|$.

Montagna *et al* (1990) and Pilla *et al* (1992) calculated the dynamic structure factor $S(\boldsymbol{q}, \omega)$ by numerically diagonalizing the dynamical matrix. They obtained results for site-percolating networks formed on 65×65 square lattices and $29 \times 29 \times 29$ cubic lattices. Stoll *et al* (1992) calculated $S(\boldsymbol{q}, \omega)$ for bond-percolating networks by a direct diagonalization technique for a 68×68 square lattice and a $21 \times 21 \times 21$ cubic lattice. Nakayama and Yakubo (1992) performed numerical calculations for $S(\boldsymbol{q}, \omega)$ for 500×500 site-percolating networks. There are some discrepancies between the different results.

Using the spectral moments method (Benoit *et al* 1992), we computed the dynamic structure factor of very large percolating clusters (bond and site), in two and three dimensions, at criticality (Rahmani *et al* 1995). We confirmed previous numerical results in agreement with the scaling behaviour theoretically predicted by Alexander *et al* (1993) in the high-frequency limit. For the low-frequency limit, we have shown that the dynamic structure factor complies with the very nice asymptotic behaviour, in agreement with theory. However, our results indicate a scaling behaviour with exponents that differ from those deduced from theory.

In this paper, we present for the first time an exhaustive study on the dynamics of the diffusion-limited cluster–cluster aggregation model. Very large aggregates of more than 10^5 particles were investigated. In several publications, we have shown that the moments methods could provide the spectral density (Royer *et al* 1992, Rahmani *et al* 1993, 1994, Thouy *et al* 1995) and correlation functions (Rahmani *et al* 1995) with good accuracy. Recently, the method was applied to the simulation of Raman scattering from fractals (Viliani *et al* 1995), and also to the study of sound wave and electromagnetic wave propagation in heterogeneous systems (Benoit *et al* 1995).

Hence, we report results of large-scale simulations of the densities of states (DOS) and the dynamic structure factors performed for three-dimensional diffusion-limited cluster–cluster aggregation. Systems of different densities are studied and our estimated values for the required scaling exponents are given.

In section 2, we describe numerical simulations of 3D DCLA system formation. In section 3, we briefly recall scaling arguments concerning the dynamic structure factor. In section 4, we present the results of our calculations of $g(\omega)$ and $S(\boldsymbol{q}, \omega)$. Finally, in section 5 we discuss our numerical results in the light of the scaling theory. Comparisons with results obtained for silica aerogels are reported.

2. The DLCA structure model

A three-dimensional DCLA lattice model was developed to simulate cases where there is a sufficiently large particle concentration to form a gelling network at the end of the aggregation process. We briefly review the method for constructing our system.

Initially, N identical particles of unit diameter are randomly disposed on the sites of a cubic lattice of unit parameter, avoiding double occupancy, within a cubic box of edge length L. The concentration c is given by

$$c = N/L^3. \tag{3}$$

At a later time, one obtains a collection of N_a aggregates, the ith aggregate containing n_i particles, so

$$\sum_{i=1}^{N_a} n_i = N. \tag{4}$$

The algorithm proceeds as follows: an aggregate i is chosen at random according to a probability p_{n_i}, which depends on the number of particles n_i that it contains, given by

$$p_{n_i} = n_i^{\alpha} \Big/ \sum_i n_i^{\alpha}. \tag{5}$$

In our simulation, we used $\alpha = -0.55$, a value close to $-1/D$ where $D = 1.78$ is the fractal dimension of the resulting three-dimensional aggregate, to make sure that the diffusion coefficient of the aggregates would vary with the inverse of their radius.

Then a space direction is chosen at random among the six directions $\pm x, \pm y, \pm z$, and an attempt is made to move the cluster rigidly by a step of one unit length in that direction. If the cluster does not collide with any other cluster during this motion, i.e. if no particle overlap occurs, the displacement is performed and the algorithm continues by again choosing a cluster at random. If, instead, a collision occurs, i.e. if a particle of one cluster tends to occupy the same position as a particle of another cluster, the displacement is not performed and the collection of clusters is updated: the two colliding clusters are discarded and a new cluster, formed by sticking the colliding clusters together, is added to the collection. After that, one cluster is again chosen at random, etc. Periodic boundary conditions are used at the edges of the box.

To illustrate the structure of our system, figure 1 shows a small simulated configuration for a 3D DLCA model formed in a box of size $L = 24$ at concentration $c = 0.15$.

The resulting configuration consists of a disordered, but homogeneous, array of fractal aggregates connected together. It has been shown (Hasmy *et al* 1994) that the mean size ξ of these aggregates decreases as the concentration c increases according to

$$\xi \sim c^{-1/(3-D)} \tag{6}$$

where D is the fractal dimension of the 3D DLCA of close to 1.8.

This simulation provides a good model for silica aerogels since, as revealed by small-angle x-ray scattering (SAXS) or small-angle neutron scattering (SANS), the materials are made up of a disordered array of connected fractal clusters resulting from primary-particle aggregations. The colloidal aerogels, which are synthesized from a silica sol, are made of quasimonodisperse spherical particles whose sizes can be determined directly from micrographs. In contrast, polymeric aerogels are prepared by chemical reactions with organosilicates. 'Basic' and 'neutral' aerogels can be distinguished according to the pH of the hydrolysis aqueous solution. Basic aerogels are made of larger-sized, but strongly polydispersed, primary particles, while particle sizes in neutral aerogels are smaller and extend down to the atomic range.

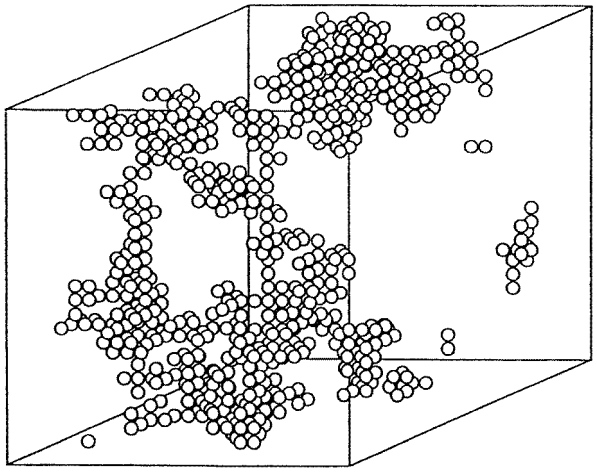

Figure 1. The configuration of the 3D DLCA aggregate built in a box of size $L = 24$ at the concentration $c = 0.15$.

3. Dynamics

Consider a 3D DLCA system consisting of N particles with unit mass and linear springs connecting two nearest-neighbour atoms. The equations for atomic motion are

$$\ddot{u} + \sum_j K_{ij} u_j = 0 \tag{7}$$

with

$$K_{ii} = -\sum_{j \neq i} K_{ij}$$

and where u_i is the displacement of the atom on the ith site.

The force constant is taken to be $K_{ij} = 1$ if the particles i and j are nearest neighbours, and $K_{ij} = 0$ if otherwise. The displacement u_i has only one component. Such a simplification does not affect the intrinsic nature of the dynamics of the present system. In ordinary numerical methods, one must diagonalize the dynamical matrix in order to calculate the eigenvalues ω_i^2 and their eigenvectors. This conventional method requires a large amount of CPU time and memory as the cluster size N becomes large. This is unsuitable for our problem because the cluster size of our systems must be very large to allow for fracton modes which are localized in the low-frequency region. Using the spectral moments method, one can determine the spectral densities, correlation functions, infrared and Raman spectra (Poussigue *et al* 1991) or inelastic neutron scattering cross-sections (Poussigue *et al* 1994), directly from the dynamical matrix.

3.1. Scaling arguments for $S(q, \omega)$

The dynamic structure factor $S(q, \omega)$ is defined by

$$S(q, \omega) = \sum_j |a_j(q)|^2 \delta(\omega - \omega_j) \tag{8}$$

with

$$a_j(q) = \sum_n q\langle n|j\rangle e^{i\boldsymbol{q}\cdot\boldsymbol{r}_n} \tag{9}$$

where $\boldsymbol{r}_n$ is the equilibrium position of the nth particle, and ω_j and $\langle n|j\rangle$ are the frequency and the nth components of the eigenvector $|j\rangle$ of the jth mode.

As noted above, Alexander (1989) and Alexander *et al* (1993) have shown that the dynamic structure factor can be expressed in terms of the scaling function $H(x)$ which complies with the power-law form

$$H(x) \sim \begin{cases} x^{\tau} & x \ll 1 \\ x^{-\tau'} & x \gg 1 \end{cases} \tag{10}$$

where τ and τ' are scaling indices which can be determined by numerical simulations. According to the SLSP (2), the dynamic structure factor $S(q,\omega)$ has the form

$$S(q,\omega) \sim \begin{cases} q^{y+\tau}\omega^{-\tau\tilde{d}/D} & q\lambda(\omega) \ll 1 \\ q^{y-\tau'}\omega^{-\tau'\tilde{d}/D} & q\lambda(\omega) \gg 1 \end{cases} \tag{11}$$

where the exponent y is given by

$$y = 2\sigma - D/\tilde{d}. \tag{12}$$

σ is the averaged strain exponent which must be greater than one; indeed, a value $\sigma < 1$ leads to a scaling breakdown (Alexander *et al* 1993). Considering $D, \tilde{d}$ and σ as the basic scaling indices, the scaling arguments applied to the dynamic structure factor $S(q,\omega)$ predict that its behaviour is as follows (Alexander *et al* 1993):

(i) *in the* $q\lambda(\omega) \ll 1$ *limit*

$$S(q,\omega) \sim q^{\gamma}\omega^{-\alpha} \tag{13}$$

where $\gamma = 4$ and $\alpha = 1 - (2\sigma - 4)\tilde{d}/D$; and

(ii) *in the* $q\lambda(\omega) \gg 1$ *limit*

$$S(q,\omega) \sim Aq^{\delta_1}\omega^{\beta_1} + Bq^{\delta_2}\omega^{\beta_2} \tag{14}$$

where $\delta_1 = 2\sigma - D$, $\beta_1 = \tilde{d} - 1$, $\delta_2 = -D$ and $\beta_2 = 2\sigma\tilde{d}/D + \tilde{d} - 1$.

So, in this limit, the asymptotic behaviour of $S(q,\omega)$ is controlled by the exponents $\tau_1' = \beta_1 D/\tilde{d}$ and $\tau_2' = \beta_2 D/\tilde{d}$.

To test the theoretical predictions, many simulation experiments have been conducted on percolating networks (Montagna *et al* 1990, Pilla *et al* 1992, Stoll *et al* 1992, Nakayama and Yakubo 1992). More recently, to clarify some discrepancies between the scaling approach predictions and numerical simulation results obtained by the different authors, we performed calculations with the dynamic structure factor $S(q,\omega)$ (Rahmani *et al* 1995). We obtained results on very large percolating clusters (bond and site), in two and three dimensions. We have shown that the scaling law of the length scale $\lambda(\omega)$ is, as expected, in agreement with 'the single-length-scale postulate' of Alexander, Courtens and Vacher. For the $q\lambda \ll 1$ limit, our results confirmed and supplemented the previous numerical results and are in agreement with the scaling behaviour theoretically deduced by Alexander, Courtens and Vacher (ACV). We obtained exponents $\tau = 3.30$ and 3.77 for 2D and 3D systems respectively. The values of the exponent σ deduced for all percolating networks are in accordance with the conclusion of ACV that $\sigma > 1$.

For the $q\lambda \gg 1$ limit, we have shown that the dynamic structure factor complies with the asymptotic behaviour $S(q,\omega) = q^{y}H(q\lambda(\omega))$, where the scaling function is a power

law, $x^{-\tau'}$. The values obtained for τ' are about 1.20 and 1.00 for the 2D and 3D percolating clusters (site and bond) respectively, which are consistent with the values obtained from the data analysis of Stoll *et al* (1992). These values do not correspond to the theoretical values given by relations (14), but are consistent with the SLSP conjecture.

In the present paper, we extended our calculations to the DLCA model, which could be useful for demonstrating the universality of the ACV assumptions and interpreting experimental results concerning silica aerogels.

4. Numerical results

We performed calculations on the density of states $g(\omega)$ and the dynamic structure factor $S(q, \omega)$ for three samples of very large on-lattice DLCA aggregates built in an $L = 100$ cubic box with periodic boundary conditions. Let us denote these samples as a, b and c, corresponding to concentrations $c = 0.05, 0.075$ and 0.15 respectively; the numbers of particles in these samples are $N = 50\,000, 75\,000$ and $150\,000$ respectively. The numerical results represent means of five a samples, three b samples and two c samples.

4.1. Densities of states

The spectral moments method could provide, with some variations, the total DOS with good accuracy. The detailed computing aspect of the method has been published elsewhere (Benoit *et al* 1992).

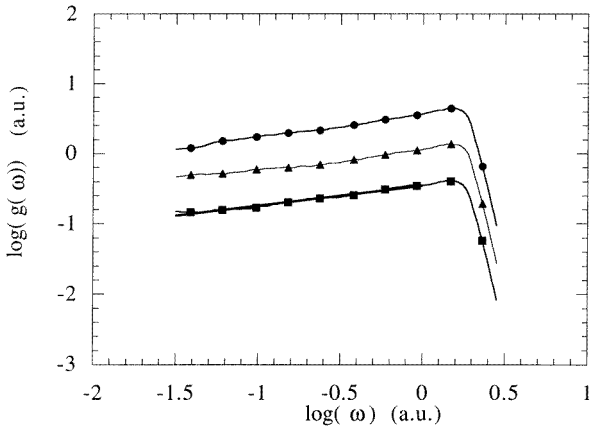

Figure 2. The DOS $g(\omega)$ versus ω, on a log–log scale, for the three 3D DLCA samples a, b and c: ——■——, $c = 0.050$; ——▲——, $c = 0.075$; ——●——, $c = 0.150$.

In figure 2, we have plotted, on a log–log scale, the DOS, $g(\omega)$, versus ω for the three samples (a, b and c). The full line is a linear fit of the DOS, and its slope is close to 0.28 ± 0.03, i.e., $\tilde{d} = 1.28 \pm 0.03$ which is a little less than the conjectured 4/3 spectral dimension of percolating clusters. We observe that the $\omega^{0.28}$-law holds even in the low-frequency region, because the lower cut-off frequency is determined from a finite size of aggregates. For the present case, one can estimate this cut-off to be less than 10^{-3}. At lower concentrations ($c < 0.2$), the aggregates have a fractal structure on a longer-range scale. For high concentrations, a fractal structure could be expected on a short-range scale.

4.2. Dynamic structure factors

For all of the samples, the spectral moments computations for the quantity $\bar{S}(q,\omega) = S(q,\omega)/q^2$ were made for 100 different wave-vector moduli $\pi/100 \leqslant q \leqslant \pi$. Then the functions were calculated in each case for 200 different frequencies $\omega_{max}/200 \leqslant \omega \leqslant \omega_{max} \approx 2.8$.

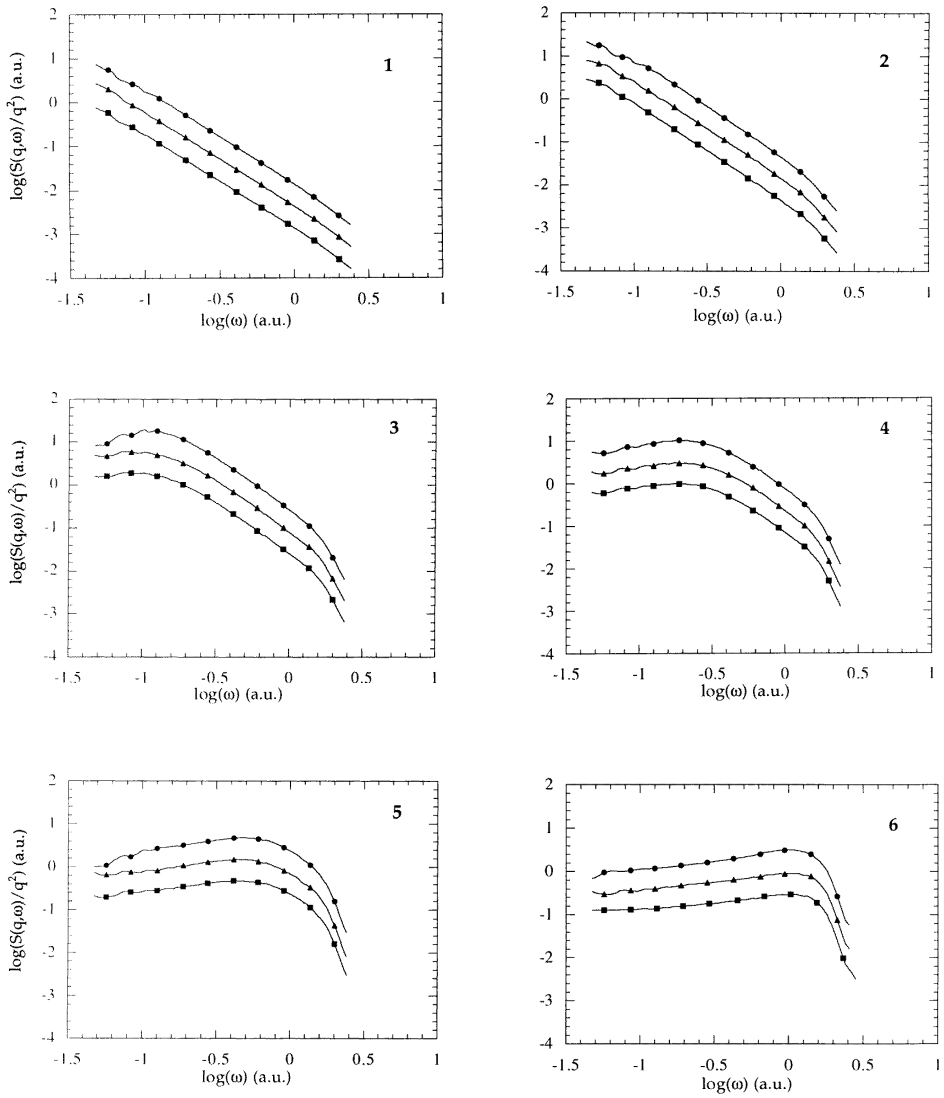

Figure 3. The reduced dynamic structure factor $\bar{S}(q,\omega) = S(q,\omega)/q^2$ versus ω, on a log–log scale, for the three 3D DLCA samples a, b and c for six fixed values of the wave-vector modulus q: (1) $q = 0.083$; (2) $q = 0.208$; (3) $q = 0.521$; (4) $q = 0.906$; (5) $q = 1.575$; (6) $q = 2.736$, and: ——■——, $c = 0.050$; ——▲——, $c = 0.075$; ——●——, $c = 0.150$.

In figure 3, we have plotted, for several q-values ((1) $q = 0.083$, (2) $q = 0.208$; (3) $q = 0.521$; (4) $q = 0.906$; (5) $q = 1.575$; (6) $q = 2.736$), the reduced dynamic

structure factor $\bar{S}(q,\omega)$ versus ω, on a log–log scale, for samples a, b and c. For each q-value, all curves exhibit the same form. As soon as q increases, a regime with a positive slope appears in the low-frequency region to the detriment of the decreasing high-frequency regime. One can distinguish two regions: $\omega \ll \omega_0$ and $\omega \gg \omega_0$, where ω_0 is the frequency at which $S(q,\omega)$ has a maximum value for each fixed wave-vector q. As $q\lambda(\omega_0) = 1$, the case where $\omega \gg \omega_0$ ($\omega \ll \omega_0$) corresponds to the $q\lambda \ll 1$ ($q\lambda \gg 1$) limit. At low q-values, the dynamic structure factor $S(q,\omega)$ is mostly dominated by a decreasing linear regime ($\omega \gg \omega_0$), whereas at substantially larger q, the linear increasing regime is dominant ($\omega \ll \omega_0$).

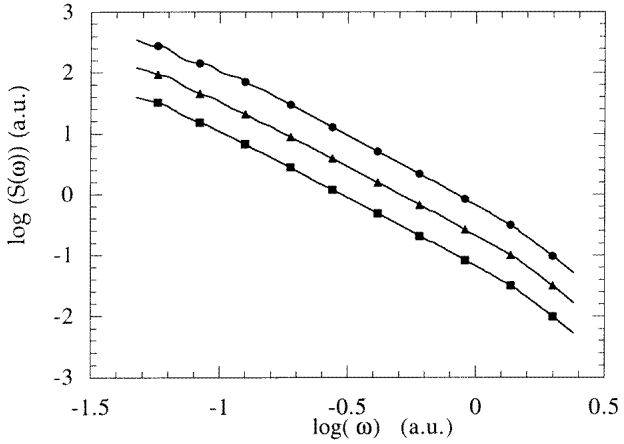

Figure 4. The global reduced dynamic structure factor $\bar{S}(\omega) = \sum_q \bar{S}(q,\omega)$ versus ω, on a log–log scale, for the three 3D DLCA samples a, b and c, in the $q\lambda \ll 1$ limit: ——■——, $c = 0.050$; ——▲——, $c = 0.075$; ——●——, $c = 0.150$.

Let us consider the asymptotic behaviour of the dynamic structure factor in the $q\lambda \ll 1$ limit. As shown in figure 4, we have plotted, on a log–log scale, the frequency dependence of a global dynamic structure factor $\bar{S}(\omega) = \sum_q \bar{S}(q,\omega)$. The curves were obtained by summing over 25 different low values of q ($\pi/100 < q < \pi/8$). This result shows that the asymptotic behaviour of $\bar{S}(\omega)$ can be expressed as $\bar{S}(\omega) \sim \omega^{-2.30\pm0.03}$ in the frequency regime $\omega \gg \omega_0$. In contrast, as shown in figure 5 ($\log(\bar{S}(\omega))$ versus $\log(\omega)$), the limit $\omega \ll \omega_0$ ($q\lambda \gg 1$) can be characterized by the power law $\bar{S}(\omega) \sim \omega^{0.40\pm0.04}$. Note also that these results are obtained by summing over 25 values of q ($\pi/2 < q < \pi$). For the three samples a, b and c, the dynamic structure factor complies with the same scaling law according to the statistical errors.

Now, as regards the wave-vector dependence of $S(q,\omega)$ given in figure 6, we have reported $S(q,\omega)$ versus q for four fixed frequencies: $\omega = 0.356$, 0.557, 0.879 and 1.103, for the heaviest sample, c. The four curves are similar in appearance, with two parts corresponding to two different q-scalings. In order to check the q-index scalings of $S(q,\omega)$, we determined, for each frequency ω, the wave-vector modulus q_0 for which $\bar{S}(q,\omega)$ has the maximum value. The values of $\bar{S}(q,\omega)$ are then rescaled by $\bar{S}(q_0,\omega)$ and averaged over ω to give the function

$$\bar{S}(q) = S(q)/q^2 = \frac{1}{n}\sum_{\omega=1}^{n}(\bar{S}(q,\omega)/\bar{S}(q_0,\omega)).$$

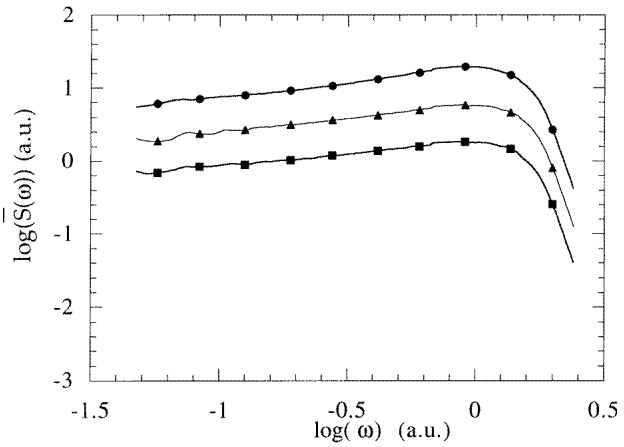

Figure 5. The global reduced dynamic structure factor $\bar{S}(\omega) = \sum_q \bar{S}(q, \omega)$ versus ω, on a log–log scale, for the three 3D DLCA samples a, b and c, in the $q\lambda \gg 1$ limit: ——■——, $c = 0.050$; ——▲——, $c = 0.075$; ——●——, $c = 0.150$.

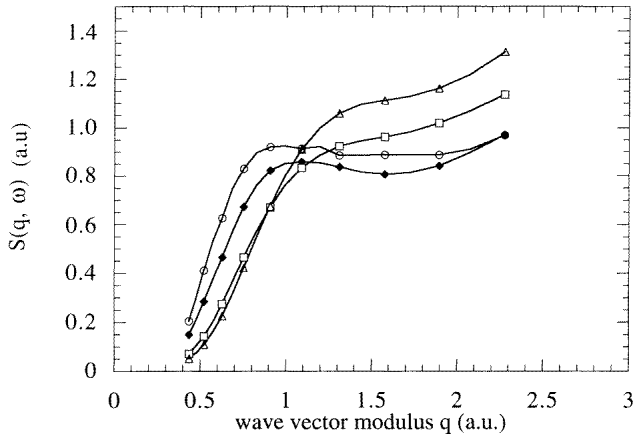

Figure 6. The dynamic structure factor $S(q, \omega)$ versus q, for the heaviest 3D DLCA sample ($c = 0.15$) for four values of frequency ω: ——○——, $\omega = 0.356$; ——♦——, $\omega = 0.557$; ——□——, $\omega = 0.879$; ——△——, $\omega = 1.103$.

We have represented in figure 7, on a log–log scale, the dependence of the function $\bar{S}(q)$ versus q/q_0 for the three samples a, b and c. In fact these curves are obtained by averaging over $n = 50$ values of ω-frequencies ($\omega_{max}/8 < \omega < \omega_{max}/2$). The results demonstrate that the wave-vector dependence complies with the power law $S(q) \simeq q^{3.90\pm0.10}$ for q below q_0 and $S(q) \simeq q^{0.21\pm0.04}$ for q above q_0.

To test the accuracy of our computed results, we plotted, on a log–log scale, the scaling function $H(q\lambda(\omega)) = q^{-y}S(q, \omega)$ versus $q\lambda(\omega)$ for the three samples (figure 8). The curves are obtained by averaging over 50 values of the wave-vector modulus q. According to the

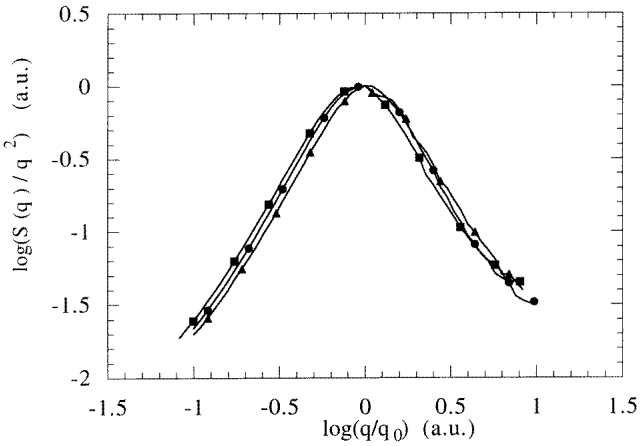

Figure 7. The average reduced dynamic structure factor

$$\bar{S}(q) = S(q)/q^2 = \frac{1}{n}\sum_{\omega=1}^{n}(\bar{S}(q,\omega)/\bar{S}(q_0,\omega))$$

(where $\bar{S}(q,\omega) = S(q,\omega)/q^2$) versus q/q_0, on a log–log scale, for the three 3D DLCA samples a, b and c: ——■——, $c = 0.050$; ——▲——, $c = 0.075$; ——●——, $c = 0.150$.

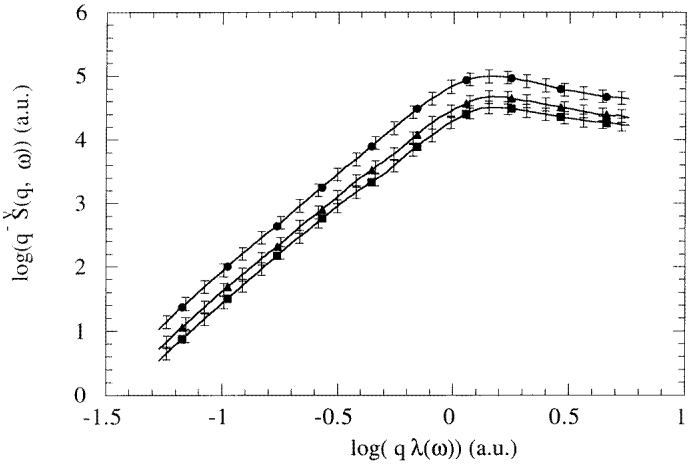

Figure 8. The scaling function $(q^{-y}S(q,\omega))$ versus $q\lambda(\omega)$, on a log–log scale, for the three 3D DLCA samples a, b and c. Bars represent statistical errors, and: ——■——, $c = 0.050$; ——▲——, $c = 0.075$; ——●——, $c = 0.150$.

results above, we find the scaling law ($x = q\lambda(\omega)$):

$$H(x) \sim \begin{cases} x^{3.1\pm0.1} & x \ll 1 \\ x^{-0.6\pm0.1} & x \gg 1. \end{cases} \tag{15}$$

Finally, the length scale is plotted versus the frequency, on a log–log scale, in figure 9, for the three samples a, b and c. As indicated by the full line, we observe that the scaling length complies with the power law: $\lambda(\omega) \sim \omega^{-0.72\pm0.03}$. From the dispersion relation

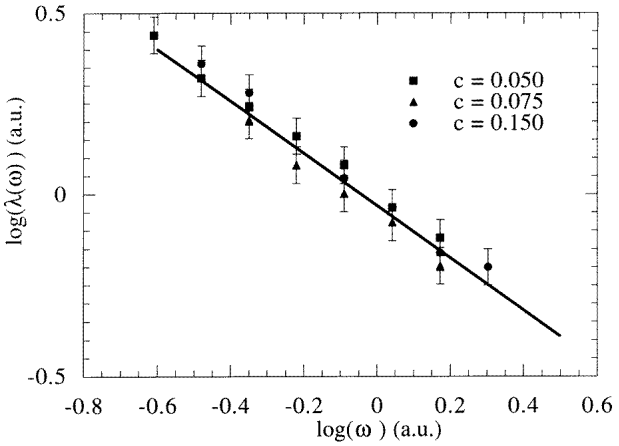

Figure 9. The values of the wavelength $\lambda(\omega)$ plotted as a function of frequency ω, on a log–log scale, for the three 3D DLCA samples a, b and c: ■, $c = 0.050$; ▲, $c = 0.075$; ●, $c = 0.150$.

$\lambda(\omega) \sim \omega^{-\tilde{d}/D}$, using the spectral dimension value $\tilde{d} = 1.28 \pm 0.03$, one deduces that the fractal dimension of our systems is $D = 1.78 \pm 0.10$. This in very close agreement with the fractal dimension $D = 1.78$ of the 3D DLCA model.

5. Discussion and conclusion

In summary, in the $q\lambda \ll 1$ limit, the results show that the dynamic structure factor complies with the power law $S(q, \omega) \sim q^{\gamma}\omega^{-\alpha}$ with $\gamma = 3.90 \pm 0.10$ and $\alpha = 2.30 \pm 0.03$. The γ-value is in complete agreement with theory (equation (13)). Using the value $\tilde{d}/D = 0.72 \pm 0.03$, one can deduce that the exponent τ defined in equation (11) is $\tau = 3.20 \pm 0.05$ ($\tau = \alpha D/\tilde{d}$), which is close to the value 3.1 ± 0.1 deduced from the scaling function in figure 8. From equation (13), one obtains $\sigma = 1.09 \pm 0.06$. This value is in agreement with the notion that $\sigma \gg 1$ (Alexander *et al* 1993).

In the $q\lambda \gg 1$ limit, we have the scaling form $S(q, \omega) \simeq q^{\delta}\omega^{\beta}$ with $\delta = 0.21 \pm 0.04$ and $\beta = 0.40 \pm 0.04$. These values differ slightly from the theoretical values of $\delta_1 = 0.40 \pm 0.20$ and $\beta_1 = 0.28 \pm 0.03$ (and differ strongly from the other theoretical values $\delta_2 = -1.8 \pm 0.1$ and $\beta_2 = 1.9 \pm 0.2$) (equation (14)). We also note the coherence of our exponent calculations with respect to the q-dependence and frequency dependence of the dynamic structure factor. For example, $\tau'(\beta) = \beta D/\tilde{d} = 0.57 \pm 0.08$ is in close agreement with $\tau'(\delta) = y - \delta = 0.60 \pm 0.15$ as well as with the value 0.6 ± 0.1 deduced from the scaling function H (equation (15)).

Note, as mentioned by Alexander *et al* (1993), that equation (14) can be written in terms of the supplementary indices z_1 and z_2 as

$$S(q, \omega) \sim Aq^{\delta_1 + z_1}\omega^{\beta_1 - z_1\tilde{d}/D} + Bq^{\delta_2 + z_2}\omega^{\beta_2 - z_2\tilde{d}/D}. \tag{16}$$

If we suppose that in this limit ($q\lambda \gg 1$), the dynamic structure factor is controlled by the exponent $\tau'_{1(theo)} = 0.40 \pm 0.04$, i.e. separate motion of blobs, by comparison with the computed values of δ and β, we find $z_1(\delta) = -0.21$ from the q-dependence and $z_1(\beta) = -0.17$ from the frequency dependence. If we assume that the second contribution resulting from the internal strain of the blob is dominant, one obtains $z_2(\delta) = 1.99$ from the

q-dependence and $z_2(\beta) = 2.03$ from the frequency dependence. We note the agreement of the computed exponents z_1 and z_2 obtained from the q- and ω-dependences respectively.

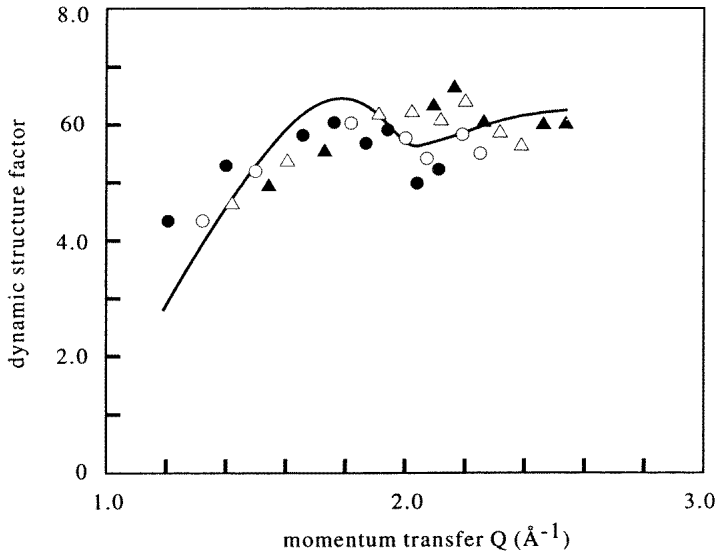

Figure 10. Experimental and theoretical (full line) dynamic structure factors for different frequencies, for a basic aerogel of density 250 kg m^{-3} (after Reichenauer *et al* 1989): ●, 0.09 THz; ▲, 0.70 THz; ○, 0.260 THz; ■, 1.070 THz; △, 0.45 THz.

Vibration excitations in base-catalysed silica aerogels of different densities have been investigated by inelastic neutron scattering. The fractal dimension of these systems is about $D = 1.8$. In figure 10, we reproduce, from Reichenauer *et al* (1989), the experimental and theoretical (linear curve) inelastic intensity versus momentum transfer Q for a base-catalysed silica aerogel of density 250 kg m^{-3} at different frequencies: (1) 0.09 THz, (2) 0.26 THz, (3) 0.45 THz, (4) 0.70 THz and (5) 1.07 THz. Their theoretical curve was obtained by a phenomenological approach.

Comparison of our result on the dynamic structure factor with the experimental measurement of Reichenauer shows a qualitative similarity between the curves in figure 6, which represent the functions $S(q, \omega)$ versus the wave-vector magnitude q with respect to our samples c, and the curves in figure 10 for a basic aerogel of density 250 kg m^{-3}. The concentration $c = 0.15$ of our sample corresponds to the aerogel density $\rho = 172$ kg m^{-3}.

We mentioned the good agreement of the fractal dimension value $D = 1.78 \pm 0.1$ for the diffusion-limited cluster–cluster aggregation model and $D = 1.8$ for basic aerogels. The spectral dimension of these latter has been estimated from Raman scattering to be $\tilde{d} = 1.21$–1.31 (Boukenter *et al* 1987, Champagnon *et al* 1987) for a sample of density 0.09 g cm^{-3}. This also seems to be fully in line with our calculated values. However, from Brillouin scattering, the estimated spectral dimension of the base-catalysed silica aerogels is $\tilde{d} = 1.1 \pm 0.1$ (Vacher *et al* 1990, Anglaret *et al* 1994). This value has been related to tensorial elasticity. Calculations with bond-bending force models are in progress, to take into account the tensorial nature of the vibrations in realistic systems, i.e. basic aerogels.

Acknowledgment

The computations were performed at the Centre National Universitaire Sud de Calcul (Montpellier, France) on an SP2 IBM computer.

References

Alexander S 1989 *Phys. Rev.* B **40** 7953
Alexander S, Courtens E and Vacher R 1993 *Physica* A **195** 286
Alexander S and Orbach R 1982 *J. Physique Lett.* **43** L625
Anglaret E, Hasmy A, Courtens E, Pelous J and Vacher R 1994 *Europhys. Lett.* **28** 591
Benoit C, Poussigue G, Rousseau V, Lakhliai Z and Chenouni D 1995 *Modelling Simul. Mater. Sci. Eng.* **3** 161
Benoit C, Royer E and Poussigue G 1992 *J. Phys.: Condens. Matter* **4** 3125
Botet R, Jullien R and Kolb M 1983 *J. Phys. A: Math. Gen.* **17** L75
Boukenter A, Champagnon B, Dumas J, Duval E, Quinson J F and Serughetti J 1987 *J. Non-Cryst. Solids* **95+96** 1189
Champagnon B, Duval E, Boukenter A, Serughetti J and Dumas J 1987 *Diffusion Defect Data* **53–54** 375
Courtens E, Pelous J, Phalippou J, Vacher R and Woignier T 1987 *Phys. Rev. Lett.* **58** 128
Courtens E, Vacher R, Pelous J and Woignier T 1988 *Europhys. Lett.* **6** 245
Foret M 1992 *Thesis* Montpellier University
Hasmy A, Anglaret A, Foret M, Pelous J and Jullien R 1994 *Phys. Rev.* B **50** 6006
Hasmy A, Foret M, Pelous J and Jullien R 1993 *Phys. Rev.* B **48** 9345
Jullien R and Botet R 1987 *Aggregation and Fractal Aggregates* (Singapore: World Scientific)
Kolb M, Botet R and Jullien R 1983 *Phys. Rev. Lett.* **51** 1123
Meakin P 1983 *Phys. Rev. Lett.* **51** 1119
Montagna M, Pilla O, Viliani G, Mazzacurati V, Roucco G and Signorelli G 1990 *Phys. Rev. Lett.* **65** 1136
Nakayama T and Yakubo K 1992 *J. Phys. Soc. Japan* **61** 2601
Nakayama T, Yakubo K and Orbach R 1994 *Rev. Mod. Phys.* **66** 381
Pilla O, Viliani G, Montagna M, Mazzacurati V, Ruocco G and Signorelli G 1992 *Phil. Mag.* B **65** 243
Poussigue G, Benoit C, Sauvajol J L, Lere-Porte J P and Chorro C 1991 *J. Phys.: Condens. Matter* **3** 8803
Poussigue G, Benoit C, de Boissieau M and Currat C 1994 *J. Phys.: Condens. Matter* **6** 659
Rahmani A, Benoit C and Poussigue G 1993 *J. Phys.: Condens. Matter* **5** 7941
——1994 *J. Phys.: Condens. Matter* **6** 1483
——1995 *J. Phys.: Condens. Matter* **7** 8903
Reichenauer G, Fricke J and Buchenau U 1989 *Europhys. Lett.* **8** 415
Russ S, Roman H E and Bunde A 1991 *J. Phys.: Condens. Matter* **3** 4797
Royer E, Benoit C and Poussigue G 1992 *J. Phys.: Condens. Matter* **4** 561
Stoll E, Kolb M and Courtens E 1992 *Phys. Rev. Lett.* **68** 2472
Thouy R, Jullien R and Benoit C 1995 *J. Phys.: Condens. Matter* **7** 9703
Tsujimi Y, Courtens E, Pelous J and Vacher R 1988 *Phys. Rev. Lett.* **60** 2757
Vacher R, Woignier T, Pelous J and Courtens E 1988 *Phys. Rev.* B **37** 6500
Vacher R, Courtens E, Coddens G, Heidemann A, Tsujimi Y, Pelous J and Foret M 1990 *Phys. Rev. Lett.* **65** 1008
Viliani G, Dell'Anna R, Pilla O, Montagna M, Roucco G, Signorelli G and Mazzacurati V 1995 *Phys. Rev.* B **52** 3346